

Large-scale QRPA calculation of $E1$ -strength and its impact on the neutron capture cross section

S. Goriely¹, E. Khan²

¹*Institut d'Astronomie et d'Astrophysique, ULB - CP226, 1050 Brussels, Belgium*

²*Institut de Physique Nucléaire, IN2P3-CNRS, 91406 Orsay, France*

Abstract

Large-scale QRPA calculations of the $E1$ -strength are performed as a first attempt to microscopically derive the radiative neutron capture cross sections for the whole nuclear chart. A folding procedure is applied to the QRPA strength distribution to take the damping of the collective motion into account. It is shown that the resulting $E1$ -strength function based on the SLy4 Skyrme force is in close agreement with photoabsorption data as well as the available experimental $E1$ strength at low energies. The increase of the $E1$ -strength at low energies for neutron-rich nuclei is qualitatively analyzed and shown to affect the corresponding radiative neutron capture cross section significantly. A complete set of $E1$ -strength function is made available for practical applications in a table format for all $8 \leq Z \leq 110$ nuclei lying between the proton and the neutron drip lines.

Key words: NUCLEAR REACTIONS: QRPA, $E1$ -strength, Nuclear forces

PACS: 24.30.Cz, 21.30.-x, 21.60.Jz, 24.60.Dr

1 Introduction

The radiative neutron captures by exotic nuclei are known to be of fundamental importance in the rapid neutron-capture process (or r-process) invoked to explain the origin of approximately one half of the nuclides heavier than iron observed in nature. The r-process is believed to take place in environments characterized by high neutron densities ($N_n \gtrsim 10^{20} \text{ cm}^{-3}$), so that successive neutron captures can proceed into neutron-rich regions well off the β -stability valley. If the temperatures or the neutron densities characterizing the r-process are low enough to break the $(n, \gamma) - (\gamma, n)$ equilibrium, the r-abundance distribution depends directly on the neutron capture rates by the so-produced exotic neutron-rich nuclei [1]. The neutron capture rates are commonly evaluated within the

framework of the statistical model of Hauser-Feshbach. This model makes the fundamental assumption that the capture process takes place with the intermediary formation of a compound nucleus in thermodynamic equilibrium. In this approach, the Maxwellian-averaged (n, γ) rate at temperatures of relevance in r-process environments strongly depends on the electromagnetic interaction, i.e the photon de-excitation probability.

The photon transmission coefficient from a compound-nucleus excited state is dominated by the $E1$ transition which is classically estimated within the Lorentzian representation of the giant dipole resonance (GDR), at least for medium- and heavy-mass nuclei. Reaction theory relates the γ -transmission coefficient for excited states to the ground state photoabsorption assuming the giant resonance to be built on each excited state. Experimental photoabsorption data confirms the simple semi-classical prediction of a Lorentzian shape at energies around the resonance energy E_{GDR} . For this reason, for practical applications involving neutron-capture cross section calculations, the $E1$ -strength function is exclusively estimated so far on the basis of a form or another of the Lorentzian model. To explain the measured strength functions and γ -ray intensities [2], it is however required to bring correction to the low-energy behavior of the strength. This is achieved by introducing an energy-dependent width [2] or an energy- and temperature-dependent width [1,3,4] guided by more detailed finite Fermi system descriptions [5] of the $E1$ -strength function at energies below the neutron separation energy S_n . These corrections were shown to improve significantly the predictions of the experimental radiation widths and gamma-ray spectra [1,6].

In addition to the generalized Lorentzian model [1,4,6], improved description of the $E1$ -strength function can be derived from the semi-classical thermodynamic pole approach [7], the microscopic random phase approximation (RPA) calculations (based on Hartree-Fock [8] or relativistic mean field [9] ground state descriptions) or the theory of finite Fermi systems [5]. None of the so-called microscopic approaches provides at the moment a complete set of $E1$ -strength function for practical applications, so that global predictions for unknown nuclei can only be taken from phenomenological approximation of Lorentzian type. However, extrapolating these approximations (including the location of the resonance energy) to exotic neutron-rich nuclei might not be reliable. In particular, Catara et al. [8] showed in the framework of RPA calculations that the neutron excess affects the spreading of the isovector dipole strength, as well as the centroid of the strength function. The energy shift is found larger than the one accounted by the usual $A^{-1/6}$ or $A^{-1/3}$ dependence given by the phenomenological liquid drop approximations. Various calculations [8–11] on the exotic neutron-rich nuclei predict that the existence of a neutron mantle could introduce a new type of collective mode corresponding to an out-of-phase vibration of the neutron-proton core against the neutron mantle. The restoring force for this soft dipole vibration is predicted to be smaller than that of the GDR. The total $E1$ strength in this so-called pygmy resonance (PR) is small (around a few percent of the total GDR strength), but, if located well below the neutron separation energy, can significantly increase the radiative neutron capture cross section [1]. Van Isacker et al. [10] estimated the PR energy and strength relative to that of the GDR within the incompressible fluid model of Goldhaber-Teller, assuming the dynamics of the dipole oscillations to be governed by the neutron-

proton interaction. Such calculations were then systematically applied to all the neutron-rich nuclei and shown to affect significantly (up to factors of about 100) the neutron capture rates of the $2 \lesssim S_n[\text{MeV}] \lesssim 4$ closed shell nuclei [1]. Large uncertainties in the description of the PR (in particular its energy and strength) remain and only more fundamental descriptions could shed light on its existence, as well as its relative importance and impact on neutron capture rates. In addition, different measurements suggest that some particular enhancement of the $E1$ -strength could be located at low energies even on stable nuclei, a feature that cannot be predicted by the phenomenological approach. In particular, dipole transitions to bound states investigated by means of the nuclear resonance fluorescence confirmed the systematic existence of a pygmy $E1$ -resonance at energies below the neutron separation energy [12]. PR are observed in fp -shell nuclei as well as in heavy spherical nuclei near closed shells (Zr, Mo, Ba, Ce, Sn and Pb).

For various type of applications, and more particularly for nucleosynthesis applications, but also accelerator driven systems, a great effort must be made to improve the reliability of the $E1$ -strength predictions, in particular for experimentally unreachable nuclei and in the low-energy region (typically below the neutron separation energy). Generally speaking, the more microscopic the underlying theory, the greater will be one's confidence in the extrapolations out towards the neutron-drip line, provided, of course, the predictions are capable of reproducing experimentally known data with a sufficient degree of accuracy. For this reason, use should be made preferentially of microscopic or semi-microscopic global predictions based on sound and reliable nuclear models which, in turn, can compete with more phenomenological highly-parameterized models in the reproduction of experimental data. Microscopic approaches (like the RPA) are almost never used for practical applications, because of the numerical difficulty associated with large-scale predictions and the fine tuning of the model to reproduce accurately experimental data, especially when considering a large data set. We present here the first attempt to construct a complete set of $E1$ -strength function derived from Quasi-particle RPA (QRPA) calculations based on an effective nucleon interaction of Skyrme-type. In Sect. 2, the QRPA calculations are presented. Different Skyrme interactions are compared in their predictions of the $E1$ -strength and GDR energies. In Sect. 3, the QRPA shortcoming in broadening the $E1$ -strength is cured by folding the QRPA strength on a Lorentzian-type function. A folding prescription is provided to reproduce experimental photoabsorption and available experimental $E1$ strengths at low energies, in particular average resonance capture (ARC) data. Section 4 is devoted to the analysis of exotic neutron-rich nuclei and the impact of the newly-determined strength on the neutron-capture cross sections and rates of interest for astrophysical applications. Conclusions are given in Sect. 5

2 QRPA calculations of the $E1$ -strength

Microscopic models based on the RPA are well known for their accuracy to describe collective modes such as giant resonances [13]. Due to the mean field approximation, they are able to calculate the strength function on the whole nuclear mass range in a short amount

of time. An improved RPA model is the QRPA which takes the pairing effect into account. This effect is expected to be important for open-shell nuclei. In our case the ground state is calculated with a Hartree-Fock+BCS (HF+BCS) model. It should be noted that it is the first time that large scale calculations on more than 6000 nuclei are performed in order to calculate not only their ground state (with HF+BCS) but also their excited states (with the QRPA). This allows to characterize the structure model on the whole nuclear chart, with the effective nucleon-nucleon interaction as only input, and opens the exciting perspective to study the properties of the effective interaction with respect to the nuclear excitations. However the BCS approximation is known to not properly describe the pairing correlation for many drip-line nuclei [14]. Ideally, for very neutron-rich nuclei along the drip-line, the model should take into account the coupling between the nuclear mean-field, the pairing and the particle continuum. Different approaches, such as the coordinate space HFB theory [15] or the continuum QRPA equations derived from the Time-Dependent-HFB theory [16,17] have been developed. However, large-scale calculations with such sophisticated continuum-QRPA models are far from being feasible at the present time. For this reason, we will restrict ourselves to the QRPA based on HF+BCS to get a qualitative insight of this approach on the neutron capture cross section by exotic neutron-rich nuclei. This study also provides interesting information on how calculated cross-sections obtained with two different approaches compare, namely the phenomenological Lorentzian (exclusively used nowadays in cross section calculation) and the microscopically rooted QRPA.

The QRPA model here employed [18] has already been successful in describing low-lying collective states in the oxygen [19], sulfur and argon [20] isotopic chains. The main feature of this model is its self-consistency in the sense that the mean field and the residual interaction are calculated from the same Skyrme effective interaction. The ground state is calculated within the HF+BCS approximation. The HF and the BCS equations are both solved in a self-consistent procedure. The only inputs to the calculations are the Skyrme interaction and the value of the constant pairing gap Δ . For the sake of simplicity, we choose a gap given by [21]:

$$\Delta = 12 A^{-\frac{1}{2}} \text{MeV} . \quad (1)$$

Because of the constant gap approximation we use a cutoff beyond which subshells do not participate to the pairing effect. This cutoff was chosen to take into account all the subshells of the major shell where the Fermi level belongs to. The pairing gap (1) is also used for magic nuclei. In this case the effect is not important because of the large shell spacing, so that the giant dipole resonance strength is not affected. Note that the present calculation with constant pairing gap is self-consistent only in the particle-hole channel, but not in the particle-particle channel. On top of the HF+BCS ground state, the excited $J^\pi=1^-$ states are calculated within the QRPA model. The QRPA equations are solved in the configuration space so as to exhaust the energy weighted sum rule (EWSR). All QRPA calculations are performed in the spherical approximation. The deformation effects are introduced in a phenomenological way as explained in Sect. 3. The results on strongly deformed nuclei should therefore be taken with circumspection. In E1-strength calculations a well-known spurious state appears, which corresponds to a translation of the whole

nucleus. In our case, since we do not use a projection method or a modified operator, the spurious state is unambiguously identified in each $E1$ -strength calculation : it lies close to 0 MeV (in a range between 0 and 2 MeV) and takes almost all the isoscalar strength (around 90%). Once identified this state is eliminated from the $E1$ -strength.

The most significant observable to check the validity of the model and the accuracy of the interaction is the GDR energy. Several Skyrme forces have been used, namely SIII [22], SGII [23], SLy4 [24] and MSk7 [25]. In all cases, the pairing interaction is treated within the simple above-described prescription (Eq. (1)). In order to select the most adequate interaction to the $E1$ calculations, we compare the calculated centroid and measured GDR energies for 48 spherical nuclei [26]. The root mean square deviations between the calculated centroid and measured energies are, respectively, 2267 keV for SIII, 573 keV for SGII, 457 keV for SLy4 and 564 keV for MSk7. The results are accurate for SGII, SLy4 and MSk7 interactions, as shown in Fig. 1 for the specific case of SLy4. Except for the lightest ($A \lesssim 80$) nuclei, all GDR energies are predicted within a few hundred keVs. On this basis we decide to use SLy4 for the large-scale calculation of the $E1$ -strength and the corresponding radiative neutron capture. However, it should be noted that the agreement obtained with MSk7 is also good, although for some given nuclei (in particular ^{130}Te and ^{133}Cs) the GDR energy is larger than the experimental value by more than 1 MeV. This force has an effective mass of $M^*/M=1.05$ and was fitted exclusively to the experimental masses of 1888 nuclei, with a root mean square error of 738 keV [25]. This result shows that an effective interaction like MSk7 characterized by a relatively large isoscalar and isovector effective mass (both equal to 1.05 of the nucleon mass) can reproduce the nuclear mass as well as GDR data. A low isovector effective mass of $M_v^*/M \simeq 0.70$ might therefore not be a necessary condition to reproduce photoabsorption cross sections in contrast to [27].

3 Folding procedure of the $E1$ -strength

As explained in Sect. 2, the QRPA provides an accurate description of the GDR centroid and the fraction of the EWSR exhausted by the $E1$ mode. However, it is necessary to go beyond this approximation scheme in order to describe the damping properties of the collective motion. The GDR is known experimentally to have a large energy width and therefore a finite lifetime. Different microscopic theories exist (see e.g [28–30]). However, we will restrict ourselves, for the sake of simplicity and applicability to large-scale calculations, to an empirical broadening of the GDR. Such a broadening is obtained by folding the QRPA strength by a normalized Lorentzian function. Different types of Lorentzian functions as well as prescription for the Lorentzian width are considered. The folding prescription significantly affects the extrapolation of the $E1$ -strength at low energies. In these conditions, ARC data at low excitation energies are of particular interest to constrain the folding procedure. The $E1$ -strength is finally obtained by broadening each QRPA resonance

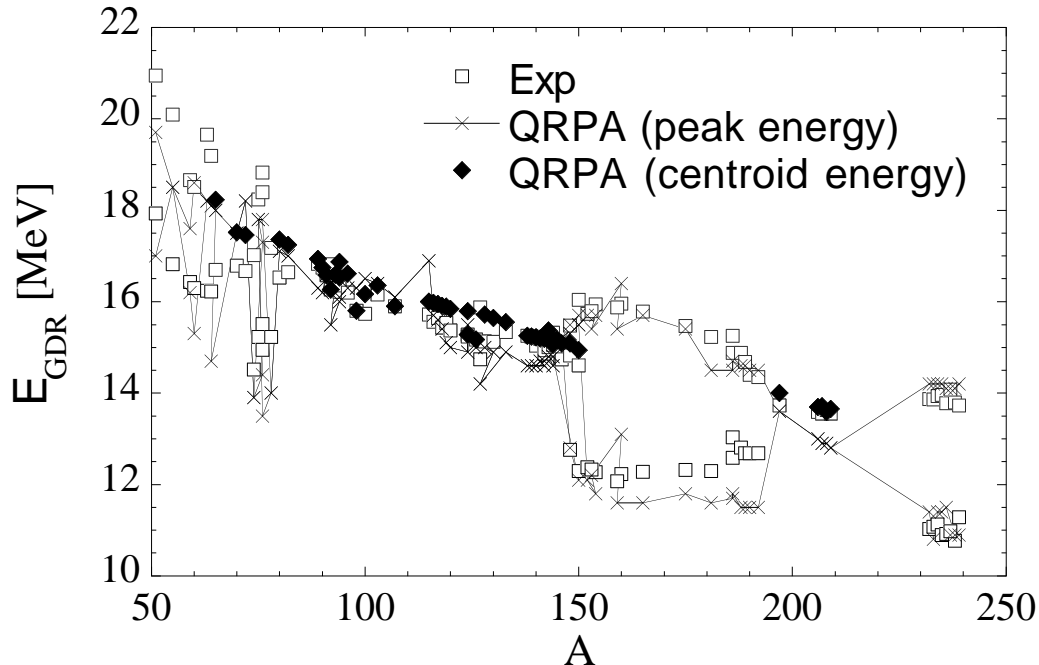


Fig. 1. Comparison between the experimental GDR energies [26] and the QRPA calculations obtained with the SLy4 Skyrme force. The QRPA centroid energies (diamonds) are displayed for 48 spherical nuclei only. The experimental GDR energies for spherical and deformed nuclei are also compared with the GDR peak energies (crosses) obtained after folding the QRPA distribution and including the deformation effects.

strength at an energy E_i by the normalized Lorentzian function

$$f_L(E, E_i, \gamma_i) = \frac{2}{\pi} \frac{\gamma_i E^2}{(E^2 - E_i^2)^2 + \gamma_i^2 E^2} . \quad (2)$$

A width $\gamma_i = \Gamma_{GDR}/2$ (where the GDR width Γ_{GDR} is taken from experimental data [26] when available or, otherwise, from empirical systematics [1,31]) is found to lead to results in good agreement with experimental GDR widths and ARC data. The resulting folded GDR peak energies obtained with the SLy4 Skyrme force are compared with experimental values in Fig. 1 for spherical and deformed nuclei (see below for the treatment of deformation). As shown in Fig. 2 in the specific case of the spherical ^{144}Nd nucleus, the ARC data for the $^{143}\text{Nd}(n,\gamma)^{144}\text{Nd}$ reaction [6] are also correctly reproduced at low energies. In addition, we compare in Fig. 3 the QRPA predictions with the compilation of experimental $E1$ strength functions at low energies ranging from 4 to 8 MeV [32] for nuclei from ^{25}Mg up to ^{239}U . The data set includes resolved-resonance measurements, thermal-captures measurements and photonuclear data. In a certain number of cases the original experimental values need to be corrected, typically for non-statistical effects, so that only values recommended by [32] are considered in Fig. 3. QRPA predictions are found to be globally in good agreement with experimental data at low energies in the whole nuclear chart and of the same degree of accuracy as the recent calculation within the thermodynamic pole approximation [7].

Note that the GDR width is expected to be temperature-dependent [33]. A temperature-

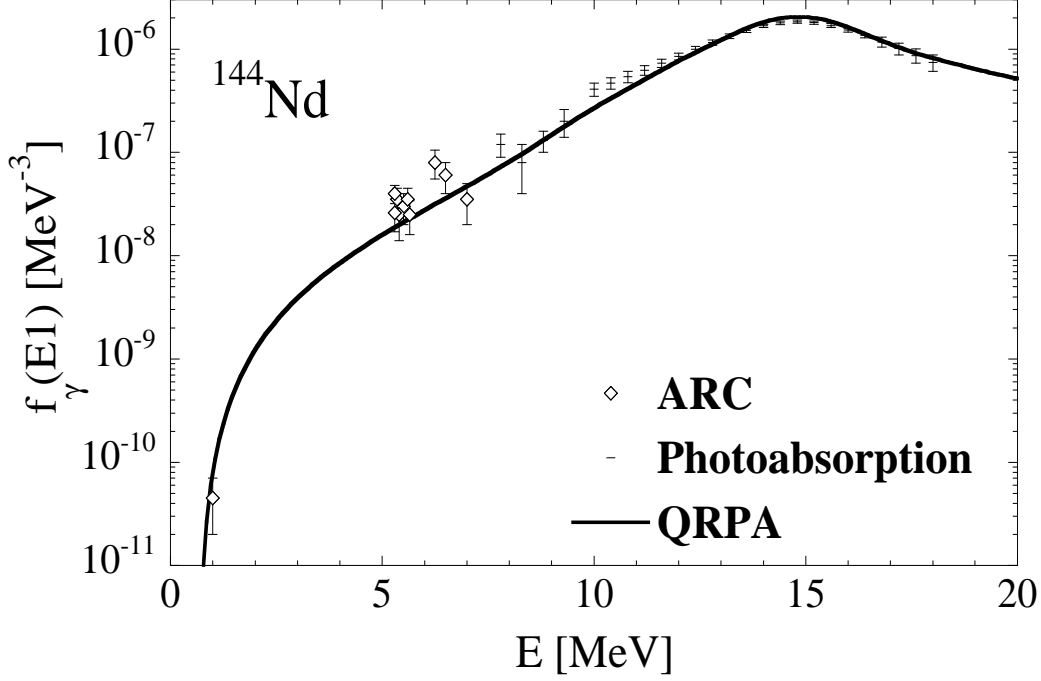


Fig. 2. Comparison of the photoabsorption data [26] and measured primary photon strength functions [6] for the $^{143}\text{Nd}(n,\gamma)$ reaction with the QRPA predictions. For the experimental data at 1 MeV, see discussion in [6]. The predictions are obtained with the SLy4 Skyrme force.

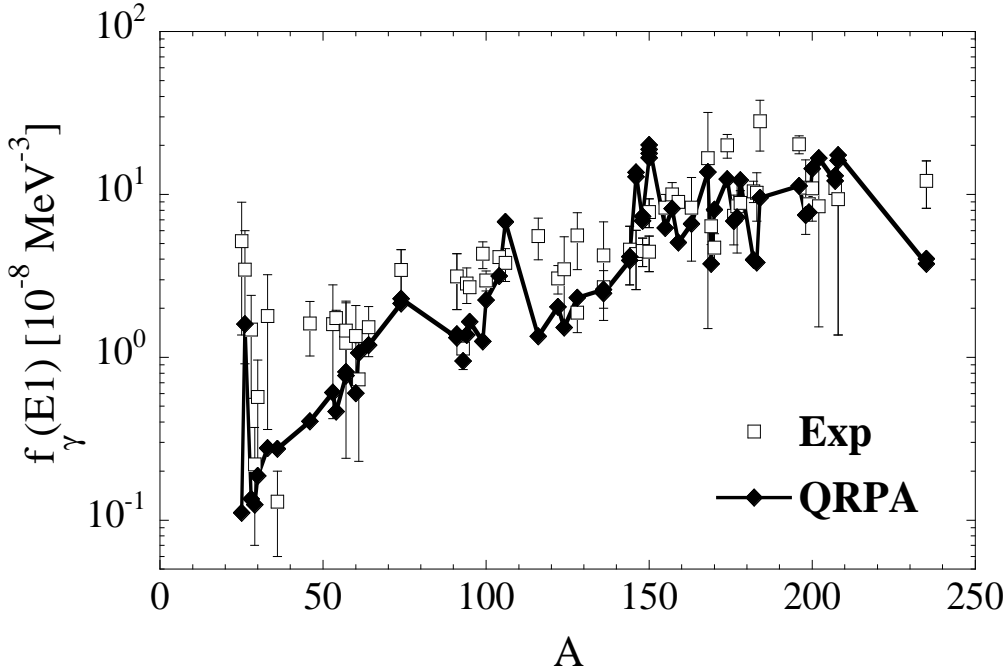


Fig. 3. Comparison of the QRPA low-energy $E1$ -strength functions with the experimental compilation [32] including resolved-resonance and thermal-captures measurements, as well as photonuclear data for nuclei from ^{25}Mg up to ^{239}U at energies ranging from 4 to 8 MeV.

dependent width γ_i affects the folded $E1$ -strength function only at high temperatures ($T \gtrsim 2$ MeV) or if some significant strength is concentrated at very low energies ($E_i \lesssim \gamma_i$), but does not influence the predictions of the low-energy data shown in Figs. 2-3. Note also that introducing a temperature-dependent spreading width γ_i in Eq. 2 does not give rise to a zero $E \rightarrow 0$ limit of the $E1$ -strength function due to the specific characteristics of the Lorentzian function considered in the folding procedure.

In the case of deformed spheroidal nuclei, the GDR is known to split into two major resonances as a result of the different resonance conditions characterizing the oscillations of protons against neutrons along the axis of rotational symmetry and an arbitrary axis perpendicular to it. In the phenomenological approach, the Lorentzian-type formula is generalized to a sum of two Lorentzian-type functions of energies E_{GDR}^l and width Γ_{GDR}^l [31], such that

$$\begin{aligned} E_{GDR}^1 + 2 E_{GDR}^2 &= 3E_{GDR} \\ E_{GDR}^2/E_{GDR}^1 &= 0.911\eta + 0.089 \end{aligned} \quad (3)$$

where η is the ratio of the diameter along the axis of symmetry to the diameter along an axis perpendicular to it. In turn, when not available experimentally, the width Γ_{GDR}^l of each peak can be expressed as a function of the respective energy E_{GDR}^l [31]. A similar splitting of the resonance strength is used in the folding procedure given by Eq. 2, each resonance energy E_i being divided with an equal strength according to Eq. 3 and characterized by a width γ_i proportional to Γ_{GDR}^l following the above-mentioned relation. Note that distributing the strength equally between the two resonance peaks (and not twice more on the high energy peak as done in the phenomelological approach) is found to give optimal location and relative strength of both centroid energies as observed experimentally. It is shown in Fig. 1 that the splitting between both energy peaks can be rather well reproduced by the present correction. The strength at low energies is supposed to be affected in a similar way, although there is no experimental indication as such. This prescription affects the low-lying strength in a way similar to the folding procedure, i.e to spread the strength around the corresponding energy.

We illustrate in Fig. 4 how the QRPA calculation reproduces the photoabsorption cross sections of four (spherical and deformed) nuclei in the whole GDR region [34]. The deformation parameter η is extracted from the HF+BCS mass calculation of [25]. In particular, the GDR energy and width, as well as the double peak structure observed experimentally are rather well reproduced by the QRPA calculation including the above-described folding and deformation prescriptions. In the case of deformed nuclei, the relative strength between both splitted peaks is also in good agreement with photonuclear data, in particular for ^{181}Ta . Note that the double peak structure in deformed nuclei, is not solely due to deformation effects, but also to a $E1$ -strength unequally distributed between 10 and 15 MeV. Although the strongest spherical QRPA peak is located around $E=13$ MeV, extra strength is found in the whole $10 \lesssim E[\text{MeV}] \lesssim 15$ energy range and is responsible for the asymmetries of the peaks. Experimentally, the $E1$ distribution is generally (at least in the

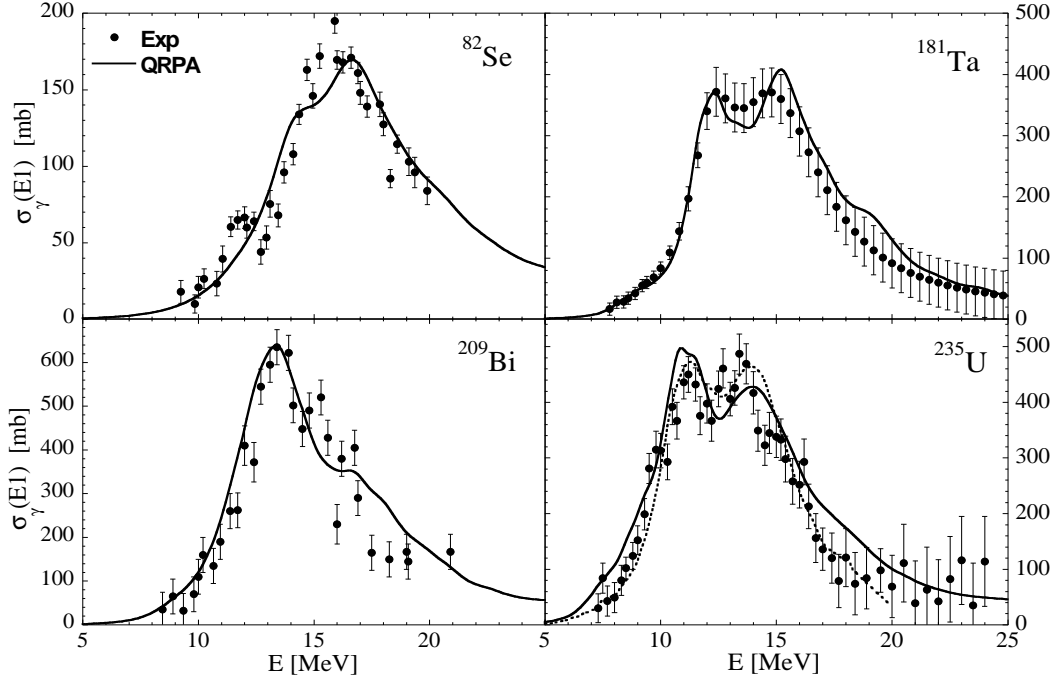


Fig. 4. Comparison of the QRPA predictions (solid line) with the experimental photoabsorption cross sections [34] for ^{82}Se , ^{181}Ta , ^{209}Bi and ^{235}U . The QRPA peak energies were slightly renormalized according to Fig. 1 to reproduce the experimental GDR energy. The dash line shown for ^{235}U corresponds to the cross section recommended by the Obninsk evaluated photonuclear library [34].

rare-earth region) characterized by a larger strength at high energies than at low energies (see e.g. ^{181}Ta). However, an inversion of this GDR strength asymmetry with a low-lying peak stronger than the high-energy one can be found in other region and is even recommended by the Obninsk evaluated photonuclear library [34], in particular for ^{234}U , ^{235}U (see Fig. 4), ^{239}Pu and ^{241}Pu . This recommended inversion, though not clearly observed in the 1976 experimental data of [35] illustrated in Fig. 4, is predicted by our QRPA calculation with the above-mentioned correction for deformed nuclei. Note that distributing unequally the strength between the two splitted peaks (for example with a strength twice larger in the high-energy state) would not reproduce as well experimental data as shown in Fig. 4.

Finally, little experimental systematics exists about the exact location and strength of the PR. Information obtained by the nuclear resonance fluorescence technique [12] suggests that the PR energy decreases with increasing masses, being around 8 MeV in the fp -shell region, 6.5 MeV around $N = 50$, $Z = 50$ and 5.5 MeV for Pb. In contrast, the PR strength increases with increasing masses, namely $B(E1) = 20 - 60$ (in $10^{-3} e^2\text{fm}^2$) for fp -shell nuclei, 70 - 90 in the $N = 50$ region, 80 - 180 in the $Z = 50$ region, and reaching 250 for ^{208}Pb . Such a systematic behavior is also found by our QRPA calculation, but the low-lying strength is located systematically some 3 MeV higher than observed. Improvements of the QRPA model based on the quasiparticle-phonon coupling could shift the PR peak energy to lower values. In particular, Colò et al. (2001) [29] found that the observed low-lying

dipole strength in the O isotopes can be explained by the QRPA plus phonon coupling model. Large-scale calculations in this framework are extremely computer-time consuming and remain to be performed.

4 Extrapolation to neutron-rich nuclei and application to the radiative neutron capture

Large-scale QRPA calculations based on the SLy4 Skyrme force (See Sect. 2) have been performed for all $8 \leq Z \leq 110$ nuclei lying between the proton and the neutron driplines, i.e some 6000 nuclei. All QRPA $E1$ -distributions are folded by a Lorentzian-type function as explained in Sect. 3, although the validity of the phenomenological folding procedure adopted in the present work cannot be confirmed at this stage. Only further improved calculations including a detailed description of the deformation and damping effects can shed light on this assumption. In the neutron-deficient region, as well as along the valley of β -stability, the resulting QRPA strength functions are very similar to the empirical Lorentzian-like approximation and therefore in good agreement with experimental photoabsorption data (Fig. 4). When dealing with neutron-rich nuclei, the QRPA predictions start deviating from a simple Lorentzian shape. In particular, some extra strength is found to be located at an energy lower than the GDR energy. The more exotic the nucleus, the stronger this low-energy component. This is illustrated in Fig. 5 for the $E1$ -strength function in the Sn isotopic chain. We should stress here that several sound nuclear models predict different behavior for the two-neutron separation energies of the Sn isotopes with $A > 132$ [36]. We present here the results for our QRPA model in order to illustrate qualitatively the role of a microscopic description of the $E1$ -strength for neutron-rich nuclei. Among the 8 distributions shown in Fig. 5, only the $A = 150$ one corresponds to a deformed configuration responsible for the double peak structure. For the $A \geq 140$ neutron-rich isotopes, an important part of the strength is concentrated at low energies ($E \lesssim 5 - 7$ MeV). However, it should be stressed that for nuclei close to the drip-line, some spurious effect may be expected due to the lack of correct continuum treatment by our model. Microscopic models such as RPA and QRPA are well suited to interpret excitations in terms of particle-hole (p-h) configurations, each configuration having a specific weight in the excited state while the pairing effects allow additional configurations with holes above the Fermi level and particles below. In this framework the low energy component arises from two distinct origins, mainly depending on the mass of the nucleus. For rather light or medium nuclei, one or two particular (p-h) configurations are found responsible for the spectacular increase of the low energy part of the $E1$ -strength in very neutron-rich nuclei such as ^{82}Ni . For heavier elements, this increase is due to more collective modes. For instance in the ^{258}Pb case, around 10 (p-h) configurations are participating to this low energy component with weights varying from 5% to 37%.

In ^{150}Sn , mainly one (p-h) configuration is participating to the low energy component with a 87% weight. Phenomenological models are unable to predict such low energy components, whatever their collectivity is. In particular for ^{150}Sn , all phenomenological systematics (as

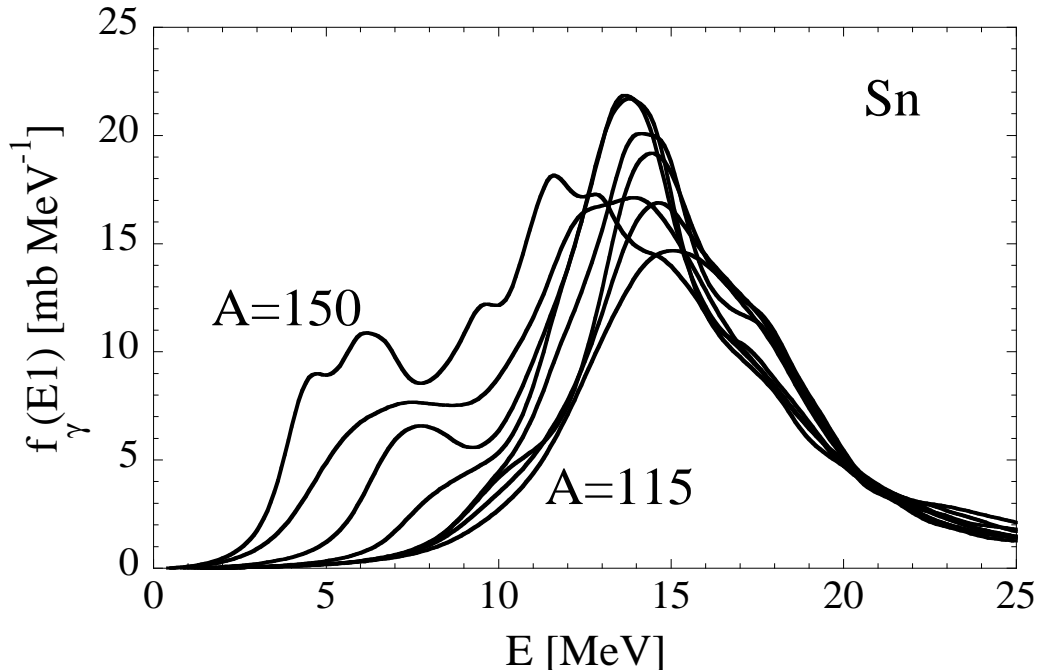


Fig. 5. $E1$ -strength function for the Sn isotopic chain predicted by the QRPA with the SLy4 Skyrme force. Only isotopes ranging between $A=115$ and $A=150$ by steps of $\Delta A=5$ are displayed.

used for cross section calculation) predict a γ -ray strength peaked around 15 MeV with a full width at half maximum of about 4.5 MeV [32] which is obviously very different from the microscopic estimate (Fig. 5). The above-described feature of the QRPA $E1$ -strength function for nuclei with a large neutron excess is found to be qualitatively independent of the adopted effective interaction. In particular, a similar enhanced strength is predicted by the MSk7 force which is characterized by a relatively large nucleon effective mass. Quantitatively, the total strength at low energies with the MSk7 interaction is smaller than in the SLy4 case.

The radiative neutron capture cross section is estimated within the statistical model of Hauser-Feshbach making use of the MOST code [37]. This version benefits in particular from an improved description of the nuclear ground state properties derived from the microscopic Hartree-Fock method [25], as well as from a reliable nuclear level density prescription based on the microscopic statistical model [38]. The direct capture contribution as well as the possible overestimate of the statistical predictions for resonance-deficient nuclei are effects that could have an important impact on the radiative neutron captures by exotic nuclei [1], but will not be included in the present analysis. We show in Fig. 6 for the Sn isotopes, the ratio of the radiative neutron capture cross section (at an arbitrary incident energy of 10 MeV exemplifying a high energy regime for which the statistical approximation of the Hauser-Feshbach model remains valid) predicted with the $E1$ -strength taken from the QRPA to the one taken from the Hybrid Lorentzian-type formula [1]. The temperature-dependent Hybrid formula corresponds to a generalization of the energy- and temperature-dependent Lorentzian formula including an improved description of the $E1$ -strength function at energies below S_n as derived from [5]. The strength of the hybrid

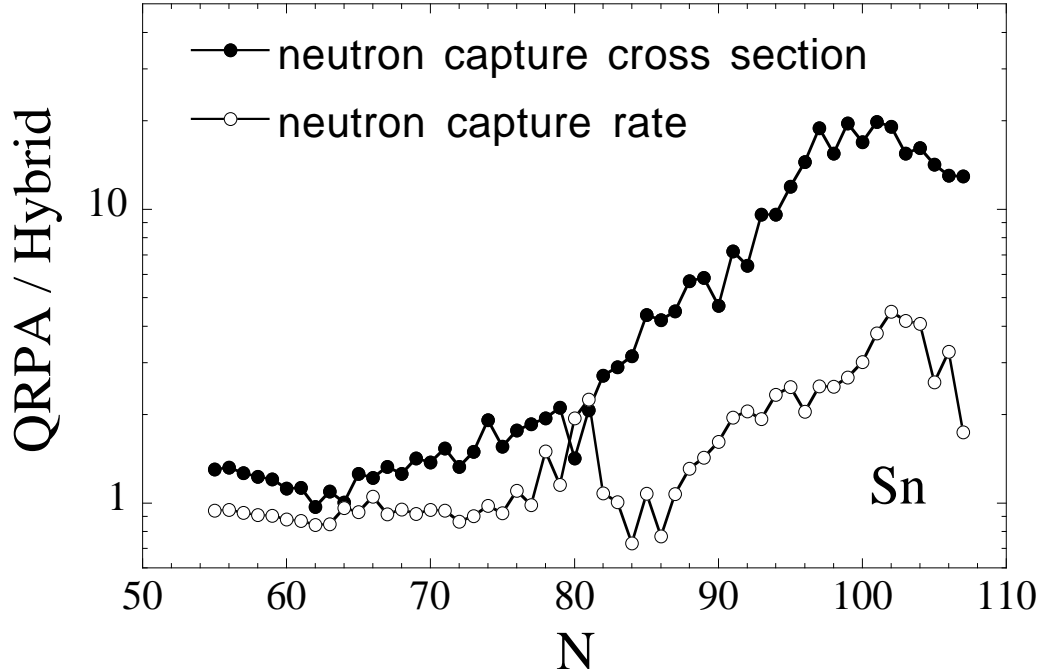


Fig. 6. Ratios of the (n, γ) cross section (full circles) and Maxwellian-averaged rate (open circles) predicted with the $E1$ -strength taken from the QRPA to the one taken from the Hybrid formula [1] for the Sn isotopes. The ratios are plotted as a function of the neutron number. The cross section is estimated at an incident energy $E = 10$ MeV and the Maxwellian-averaged rate at a temperature of $1.5 \cdot 10^9$ K.

formula differs from the QRPA estimate not only in the location of the centroid energy, but also in the low-energy tail determined by the temperature and energy-dependent width. No extra low-lying strength is included in the phenomenological Hybrid formula, but its temperature dependence increases the $E1$ strength at low energies and is responsible for its non-zero $E \rightarrow 0$ limit. The newly-derived $E1$ -strength gives an increase of the cross section by a factor up to 20 close to the neutron drip line. This is due to the shift of the GDR to lower energies compared with the usually adopted $A^{-1/3}$ rule (see Sect. 1 and Fig. 5), as well as to the appearance of the GDR strength at low energies as explained above. Both effects tend to increase the $E1$ strength at energies below the GDR, i.e. in the energy window of relevance in the neutron capture process. For less exotic nuclei, the QRPA impact is relatively small, differences being mainly due to the exact position of the GDR energy and the resulting low-energy tail, i.e. the energy-dependent width.

The Maxwellian-averaged (n, γ) rates at a temperature of $1.5 \cdot 10^9$ K characteristic of the r-process nucleosynthesis are also displayed in Fig. 6. These rates are sensitive to the neutron capture cross section at incident energies around 130 keV, and therefore depend on the $E1$ -strength in a narrow range of a few hundred keV around S_n . For nuclei with low neutron separation energies, the resonant contribution around S_n can be negligible, so that the stellar rate is principally dominated by captures of a few MeV neutrons. Deviations up to a factor of 5 are found with respect to the Hybrid formula (Fig. 6). The GDR strength predicted at low energies (see Fig. 5) is mainly responsible for the QRPA increase of the

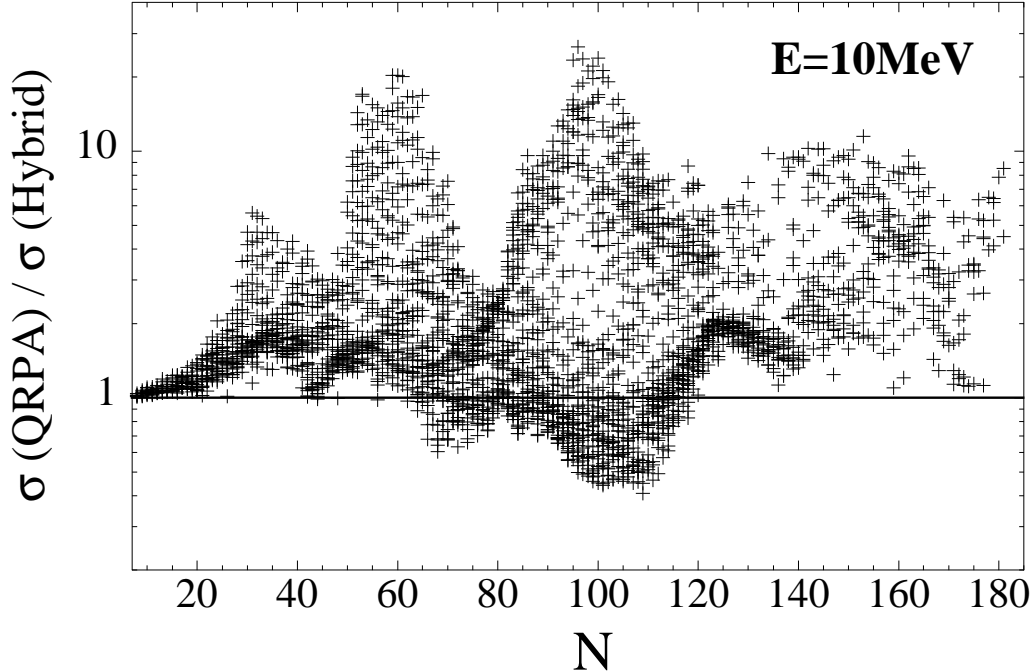


Fig. 7. Ratio of the (n, γ) cross section (at $E = 10$ MeV) predicted with the QRPA $E1$ -strength to the one derived using the Hybrid formula [1]. The figures include about 4000 nuclei with $8 \leq Z \leq 84$ lying between the neutron and the proton drip lines and are plotted as a function of the neutron number.

stellar reaction rate. In particular, below the neutron shell closure at $N = 82$, the neutron separation energy is large enough (5–7 MeV), so that the GDR tail resulting from the low-energy QRPA strength enhances the reaction rate by a factor of 2. Above $N = 82$, the neutron separation energy drops to low values ($S_n \lesssim 3$ MeV) and the reaction rates increases proportionally to the $E1$ strength shifted to lower energies for the most exotic nuclei. For example in the $^{144}\text{Sn}(n, \gamma)^{145}\text{Sn}$ case, the stellar rate and the cross section at 10 MeV are reduced by a factor of 2 and 3, respectively, if the $E1$ strength below 7 MeV is neglected (Fig. 5). These results show qualitatively the important effect the extreme neutron excess can have on the neutron capture cross section.

Similarly, the QRPA calculations have been used to estimate the neutron capture cross sections and Maxwellian-averaged rates for the 4000 nuclei with $8 \leq Z \leq 84$ lying between the neutron and the proton drip lines. They are compared in Figs. 7-8 to the predictions based on the Hybrid formula. Increases up to a factor of 30 are obtained in the cross section at 10 MeV and a factor of 8 in the rate at $1.5 \cdot 10^9$ K, in both cases for the most exotic neutron-rich nuclei. A small decrease of the neutron capture cross sections and rates can also be observed, especially in the deformed neutron-deficient region ($S_n \simeq 10$ MeV, $Z \simeq 70$ and $N \simeq 105$) where the neutron separation energy is large and the QRPA predicts, in the respective energy range of relevance, an $E1$ -strength smaller than does the Hybrid formula. In this case, the neutron capture cross section with the Hybrid formula can be up to twice larger than the one obtained with the QRPA strength. This effect is closely related to the folding procedure adopted here, leading to a zero limit of the strength function at zero

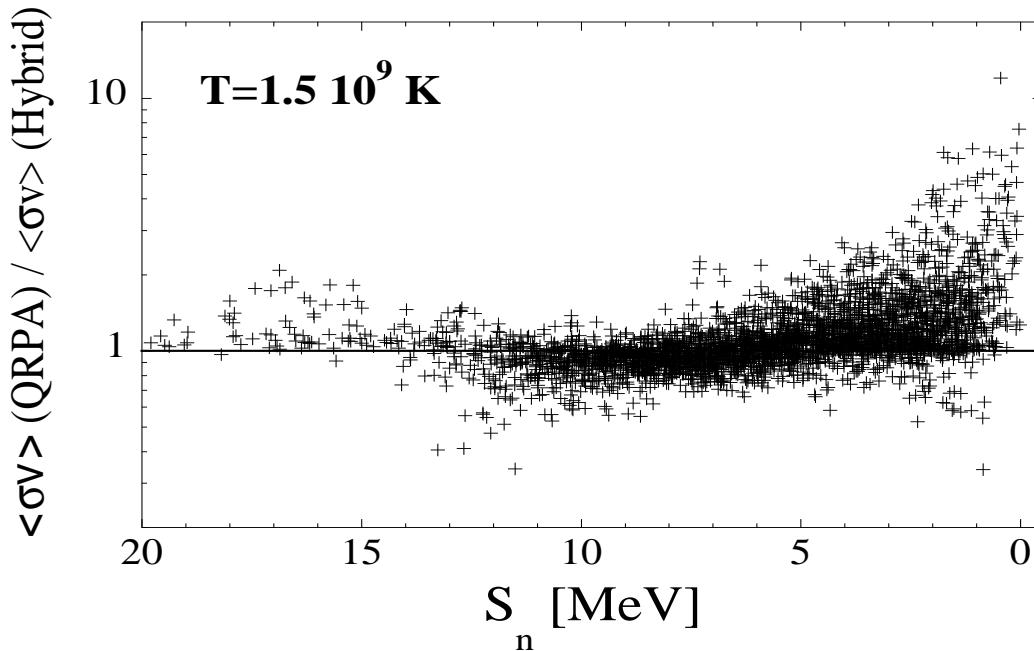


Fig. 8. Same as Fig. 7 for the Maxwellian-averaged neutron capture rate (at a temperature of $1.5 \cdot 10^9$ K) as a function of the neutron separation energy S_n .

energy in contrast to the temperature-dependence of the Hybrid prescription leading to a non-zero limit [1]. Qualitatively, similar results are obtained with the MSk7 predictions of the $E1$ -strength. Quantitatively, the increase of the neutron capture cross section by nuclei close to the neutron drip line is slightly smaller with MSk7 than with SLy4. These qualitative results points out the necessity to perform more predictive calculations, such as continuum-QRPA, to have a reliable description of nuclei along the drip-line. The impact of the newly-derived rates on the r-process nucleosynthesis will be studied in a forthcoming paper.

5 Conclusions

The total photon transmission coefficient from a compound nucleus excited state is one of the key ingredients for statistical cross section evaluation. The cross section for the radiative capture of low-energy neutrons strongly depends on the low-energy tail of the giant dipole resonance. Recent experimental and theoretical work predict a particular enhancement of the $E1$ -strength at low energies, in particular for neutron-rich nuclei. This low-energy component of the $E1$ -strength can only be derived from microscopic calculations. Microscopic descriptions of the $E1$ -strength function have become available, mainly in the QRPA approach. None of the previous QRPA calculations, however, provides a complete set of $E1$ -strength functions to be used for practical applications.

For these reasons, we present here the first attempt to construct a complete set of $E1$ -

strength function derived from QRPA calculations based on an effective nucleon-nucleon interaction of Skyrme-type. The QRPA predictions using the SLy4 Skyrme force are in close agreement with photoabsorption data. A folding procedure is applied to the QRPA strength to take the damping of the collective motion into account. A prescription for the folding procedure and for the deformation effects is proposed and shown to lead to $E1$ -strength functions in fair agreement with the available experimental data, in particular at low energies.

The folded QRPA strength is used for the evaluation of the neutron capture cross section within the framework of the statistical model of Hauser-Feshbach. The cross sections at energies around 10 MeV are found to be enhanced by a factor up to 30 when approaching the neutron drip line. The low-energy contribution to the $E1$ strength predicted by the QRPA calculations is held responsible for such an increase. No empirical prescription of the $E1$ -strength as traditionally used in reaction calculation can predict this increase of the radiative capture. This emphasizes the crucial role of nuclei along the drip-lines, and more predictive calculations in this area are called for. The neutron capture rate at temperatures of relevance to nucleosynthesis applications is however less sensitive to the GDR strength calculated here. Increase up to a factor of 8 are obtained. The QRPA strength is tabulated and made available to the scientific community via the nuclear astrophysics library at <http://www-astro.ulb.ac.be>.

Further improvements might be necessary for a better description of the low-energy tail of the GDR. In particular, the particle-vibration coupling is also known to affect the low-energy strength and could contribute to an extra increase of the radiative neutron capture rate by exotic nuclei. A more fundamental determination of the GDR width, i.e of the damping of the collective motion, as well as a more consistent treatment of deformation effects also remain to be studied in the future. A proper treatment of the pairing and the coupling to the continuum for nuclei along the drip-line is also crucial to have a quantitative idea of the increase of the neutron capture cross-sections.

Acknowledgments S.G. is FNRS Research Associate. This work has been performed within the scientific collaboration (Tournesol) between the Wallonie-Bruxelles Community and France.

References

- [1] S.Goriely, Phys. Lett. B436 (1998) 10.
- [2] C.M. McCullagh, M.L. Stelts, R.E. Chrien, Phys. Rev. C23 (1981) 1394.
- [3] Kopecky J., Chrien R.E., Nucl. Phys. A468 (1987) 285.
- [4] S.F. Mughabghab, C.L. Dunford, Phys. Lett. B487 (2000) 155.

- [5] S.G.Kadmenskii, V.P. Markushev, V.I. Furman, *Sov. J. Nucl. Phys.* 37 (1983) 165.
- [6] J.Kopecky and M. Uhl, *Phys. Rev. C*41 (1990) 1941.
- [7] V.A. Plujko, S.N. Ezhov, M.O. Kavatsyuk, A.A. Grebenyuk, R.V., Yermolenko, in : *Proceedings of Conference on Nuclear Data for Science and Technology*, (Tsukuba, Japan, 2001) in press.
- [8] F. Catara, E.G. Lanza, M.A Nagarajan, A. Vitturi, *Nucl. Phys. A*624 (1997), 449.
- [9] D. Vretenar, N. Paar, P. Ring and G.A. Lalazissis, *Nucl. Phys. A*692 (2001) 496.
- [10] P. Van Isacker, M.A. Nagarajan, D.D. Warner, *Phys. Rev. C*45 (1992) R13.
- [11] Y. Suzuki, K. Ikeda, H. Sato, *Prog. Theor. Phys.* 83 (1990) 180.
- [12] K. Govaert, F. Bauwens, J. Bryssinck, D. De Frenne, E. Jacobs, W. Mondelaers, L. Govor, V.Yu. Ponomarev, *Phys. Rev. C*57 (1998) 2229.
- [13] Nguyen Van Giai, *Prog. Theo. Phys.* 74/75 (1983) 330.
- [14] J.Dobaczewski, W.Nazarewicz, T.R.Werner, J.F.Berger, C.R.Chinn, J.Decharge, *Phys. Rev. C*53 (1996) 2809.
- [15] J.Engel, M.Bender, J.Dobaczewski, W.Nazarewicz, R.Surman, *Phys. Rev. C*60 (1999) 014302.
- [16] M. Matsuo, *Nucl. Phys. A*696 (2000) 371.
- [17] M. Grasso, E. Khan, Nguyen Van Giai and N. Sandulescu, in : *Proceedings of Conference on Yukawa International Seminar, Physics of Unstable Nuclei*, (Kyoto, Japan, 2001) in press.
- [18] E. Khan and Nguyen Van Giai, *Phys. Lett. B*472 (2000) 253.
- [19] E. Khan, Y. Blumenfeld, Nguyen Van Giai, T. Suomijärvi, N.Alamanos, F. Auger, G.Colo, N. Frascaria, A. Gillibert, T. Glasmacher, M. Godwin, K.W. Kemper, V. Lapoux, I. Lhenry, F. Maréchal, D.J. Morrissey, A. Musumarra, N.A. Orr, S. Ottini-Hustache, P. Piattelli, E.C. Pollacco, P. Roussel-Chomaz, J.C. Roynette, D. Santonocito, J.E. Sauvestre, J.A. Scarpaci, and C. Volpe, *Phys. Lett. B*490 (2000) 45.
- [20] E.Khan, T.Suomijarvi, Y.Blumenfeld, V.G.Nguyen, N.Alamanos, F.Auger, E.Bauge, D.Beaumel, J.P.Delaroche, P.Delbourgo-Salvador, A.Drouart, S.Fortier, N.Frascaria, A.Gillibert, M.Girod, C.Jouanne, K.W.Kemper, A.Lagoyannis, V.Lapoux, A.Lepine-Szily, I.Lhenry, J.Libert, F.Marechal, J.M.Maison, A.Musumarra, S.Ottini-Hustache, P.Piattelli, S.Pita, E.C.Pollacco, P.Roussel-Chomaz, D.Santonocito, J.E.Sauvestre, J.A.Scarpaci, T.Zerguerras, *Nucl. Phys. A*694 (2001) 103.
- [21] A. Bohr and B. Mottelson, *Nuclear Structure* (Benjamin, New York, 1969) Vol. 1, p. 169.
- [22] M. Beiner, H. Flocard, Nguyen Van Giai and P. Quentin, *Nucl. Phys. A*238 (1975) 29.
- [23] Nguyen Van Giai and H. Sagawa, *Nucl. Phys. A*371 (1981) 1.
- [24] E. Chabanat, P. Bonche, P. Haensel, J. Meyer, R. Schaeffer, *Nucl. Phys. A*635 (1998) 231.

- [25] S. Goriely, F. Tondeur, J.M. Pearson, 2001, *At. Data Nucl. Data Tables* 77, 311
- [26] S.S. Dietrich, B. L. Berman, *At. Data Nucl. Data Tables* 38 (1989) 199.
- [27] H. Krivine, J.Treiner and O. Bohigas, *Nucl. Phys.* A336 (1980) 155.
- [28] G. Colò, N. Van Giai, P.F. Bortignon, R.A. Broglia, *Phys. Rev C*50 (1994) 1496.
- [29] G. Colò, P.F. Bortignon, *Nucl. Phys.* A696 (2001) 427.
- [30] P. Schuck and S. Ayik, *Nucl. Phys.* A687 (2001) 220c.
- [31] F.-K. Thielemann, M. Arnould, in: *Proceedings of Conference on Nuclear Data for Science and Technology*, (eds. K. Böckhoff, Reidel, Dordrecht, 1983) 762.
- [32] Reference Input Parameter Library, IAEA-Tecdoc-1034 (1998).
- [33] P.F. Bortignon, *Nucl. Phys.* A687 (2001) 329c.
- [34] Photonuclear data for applications; cross sections and spectra, IAEA-Tecdoc-1178 (2000).
- [35] G. Gurevich, L. Lazareva, V. Mazur, G. Solodukhov, *Zh. Eksp. Teor. Fiz., Pis'ma Red.* 23 (1976) 411.
- [36] W. Nazarewicz, *Nucl. Phys.* A654 (1999) 195c.
- [37] Goriely S., 2001, in *Tours Symposium on Nuclear Physics III*, AIP Conf. Proc. 561, eds. M. Arnould et al. (New York: AIP), 53; <http://www-astro.ulb.ac.be>.
- [38] P. Demetriou and S. Goriely, *Nucl. Phys.* A695 (2001) 95.